

## Isospin mixing in $^{111}\text{In}$ and the inclusion of additional terms in the mixing formalism\*

C. R. Lux and N. T. Porile

*Department of Chemistry, Purdue University, West Lafayette, Indiana 47907*

S. M. Grimes

*Lawrence Livermore Laboratory, Livermore, California 94550*

(Received 22 December 1975)

The extent of isospin mixing in  $^{111}\text{In}$  has been determined at 20.9 MeV on the basis of measured cross sections for the  $(p, p')$ ,  $(p, \alpha)$ ,  $(\alpha, p)$ , and  $(\alpha, \alpha')$  reactions involving the formation of the  $^{111}\text{In}$  compound nucleus. The following values were obtained for the mixing fraction and the isospin mixing matrix element:  $\mu = 0.62 \pm 0.14$  and  $|H_c| = 0.013 \pm 0.004$  eV. These results are based on a reformulation of the isospin mixing theory in which additional terms are included. Previous data available for the  $A \sim 50$ –70 region are reanalyzed using this formalism and the dependence of  $|H_c|$  on energy, mass number, and the probability of proton emission from the  $T_<$  (nonanalog) states of the compound nucleus is determined.  $|H_c|$  varies inversely with the first two of these quantities and directly with the third.

NUCLEAR REACTIONS  $^{110}\text{Cd}(p, p')$  and  $(p, \alpha)$ ,  $E_p = 16.0$  MeV;  $^{107}\text{Ag}(\alpha, \alpha')$  and  $(\alpha, p)$ ,  $E_\alpha = 19.58$  MeV; measured differential cross sections at  $30^\circ$ – $150^\circ$ ; deduced isospin mixing fraction and mixing matrix element. Theory of isospin mixing reformulated to include additional terms.

### I. INTRODUCTION

The determination of isospin mixing in highly excited nuclei has been the subject of a number of recent investigations. The approach has involved a measurement of the cross sections of the  $(p, p')$ ,  $(p, \alpha)$ ,  $(\alpha, p)$ , and  $(\alpha, \alpha')$  reactions involving the formation of a particular compound nucleus. As first demonstrated by Fluss *et al.*,<sup>1</sup> isospin conservation leads to a relative enhancement in the  $(p, p')$  cross section since this is the only one of the above reactions that can proceed via the  $T_>$  (analog) states of the compound nucleus. Mixing between the  $T_>$  and  $T_<$  (nonanalog) states reduces this enhancement and the isospin mixing fraction  $\mu$  has been determined from the experimental cross sections by means of a formalism developed by Grimes *et al.*<sup>2</sup> Results of this type have been obtained for a number of nuclei in the  $A \sim 50$ –70 mass region<sup>3–7</sup> and the energy dependence of  $\mu$  has been measured for  $^{69}\text{Ga}$  (Ref. 5) and  $^{64}\text{Zn}$  (Ref. 7). Values of the isospin mixing matrix element  $|H_c|$  have been extracted from the  $\mu$  values<sup>8,9</sup> and the formalism has been reformulated<sup>9</sup> to include “upward” mixing from the  $T_<$  into the  $T_>$  states as well as the more predominant “downward” mixing.

The matrix elements extracted from the above studies appear to be correlated with both the fractional proton decay width of the  $T_<$  states,  $\Gamma_p^</\Gamma^<$ , and the mass number. However, since  $\Gamma_p^</\Gamma^<$  tends to decrease with increasing  $A$  it is difficult to unravel these two effects on the basis of data for nuclei lying in a narrow mass range.

The present work attempts to overcome this difficulty by means of a study of isospin mixing in  $^{111}\text{In}$ . This nuclide differs sufficiently in mass from the previously investigated cases to permit a determination of the mass dependence of  $|H_c|$ . In addition, we present a reformulation of the isospin mixing formalism in which additional terms in the relation between  $\mu$  and the measured cross sections are included. The resulting  $\mu$  and  $|H_c|$  are sufficiently different from those obtained by means of the simpler formalism to make it worthwhile to reanalyze all the previous data.

### II. EXPERIMENTAL

The  $^{111}\text{In}$  compound nucleus was formed at an excitation energy of 20.9 MeV by bombardment of  $^{110}\text{Cd}$  by 16.00 MeV protons and of  $^{107}\text{Ag}$  by 19.58 MeV  $^4\text{He}$  ions. The cross sections of interest were determined by measurement at various angles of the energy spectra of the emitted protons and  $\alpha$  particles. The experiments were performed with beams from the Purdue tandem Van de Graaff.

The experimental procedure has been described in detail elsewhere.<sup>10,11</sup> Briefly, the emitted charged particles were detected by a counter telescope consisting of two surface-barrier detectors. Particle identification was based on the power-law method.<sup>12</sup> Energy spectra were recorded at intervals of  $30^\circ$  between  $30^\circ$  and  $90^\circ$  and of  $20^\circ$  between  $90^\circ$  and  $150^\circ$ . Background was negligibly small in all cases. The beam intensity was determined by digitizing the current collected

in a Faraday cup attached to the beam line and was also monitored by a detector located at a fixed angle to the beam. Targets were self-supporting metallic foils having an isotopic purity of 98%.<sup>13</sup> The targets were 1.0 mg/cm<sup>2</sup> (Ag) and 1.4 mg/cm<sup>2</sup> (Cd) thick and had good uniformity, as determined by energy loss measurements performed with an  $^{241}\text{Am}$   $\alpha$  source. In performing the  $^4\text{He}$  irradiations the beam energy was adjusted to account for the slight difference in the energy lost by protons and  $^4\text{He}$  ions traversing the targets.<sup>14</sup>

### III. RESULTS

The data were processed with a number of codes to yield energy spectra and angular distributions in the c.m. system and to remove lines due to light-element impurities.<sup>15</sup> As an example of the data, Fig. 1 shows the c.m. energy spectra obtained at 150°. All the spectra feature broad evaporation peaks followed by discrete lines at the higher energies. Special attention had to be paid to the ( $\alpha, \alpha'$ ) spectra because of the presence of

an overwhelmingly intense elastic peak at the most forward angles. Slit scattering of elastic  $\alpha$  particles in the detector collimators produced a continuous background which severely distorted some of the spectra. The data were corrected for this effect on the assumption that the entire 30° spectrum could be attributed to degraded elastic  $\alpha$  particles. The correction was applied by subtracting the 30° spectrum from the other spectra after first normalizing on the elastic peak. The correction amounted to some 40% at 60° but decreased rapidly with angle, becoming  $\leq 1\%$  at backward angles.

The angular distributions of the emitted particles are shown in Fig. 2. In obtaining these data the proton spectra were integrated between 3.0 and 11.5 MeV and the  $\alpha$  spectra between 8.0 and 15.5 MeV. These energy intervals include most of the evaporation peaks while excluding all the discrete lines. The indicated uncertainties are a measure of the relative errors and are primarily due to those arising from removal of impurity lines, to differences between Faraday cup and monitor de-

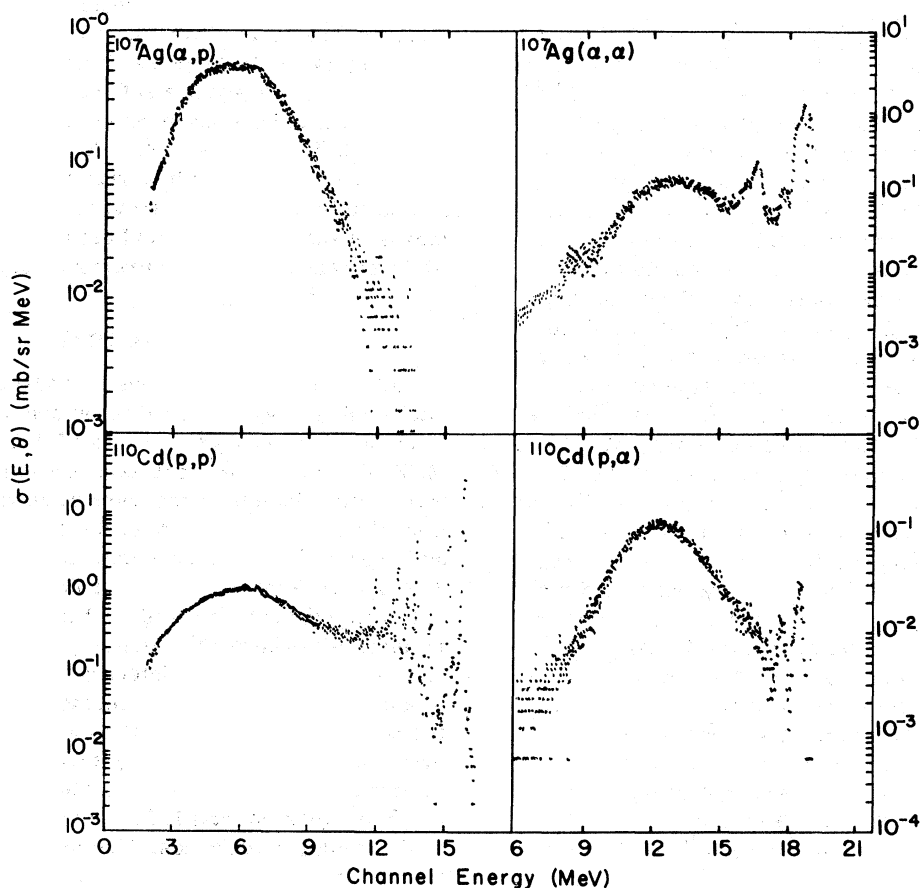


FIG. 1. Energy spectra (c.m.) of protons and  $\alpha$  particles emitted at 150° (lab) in the decay of the  $^{111}\text{In}$  compound nucleus.

tector values for the beam intensity, and in the case of the  $(\alpha, \alpha')$  reaction, to corrections for the elastic contribution. The differential cross sections are in most instances independent of angle in the backward direction but do show a substantial degree of forward peaking. This feature arises from direct or precompound processes and must be excluded in a determination of the compound nuclear cross sections.

Evaporation cross sections for the four reactions were obtained by integration of the differential cross sections over angle. It was assumed that the angular distributions were isotropic and the results are based on a least squares fit to the data at  $90^\circ$ – $150^\circ$ . In the case of the  $(\alpha, \alpha')$  reaction only the  $130^\circ$  and  $150^\circ$  spectra were used because of the forward peaking observed at smaller angles. The results are summarized in Table I, where the listed uncertainties include the standard deviations in the least-squares fits as well as estimated uncertainties in target thickness (3%) and detector geometry (2%).

Previous studies<sup>3-7</sup> of reactions induced by low-energy protons and  $^4\text{He}$  ions have shown that the  $(p, p')$  reaction, alone among the reactions of

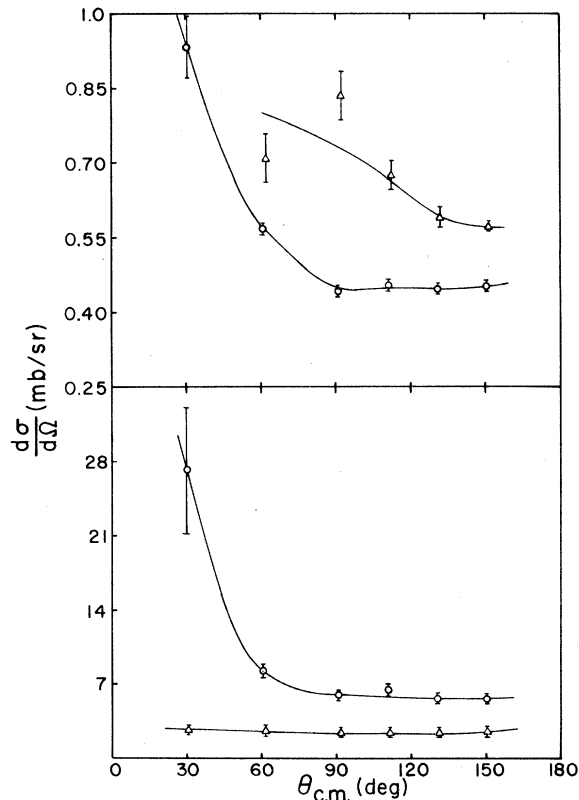


FIG. 2. Angular distribution of  $\alpha$  particles (top panel) and protons (bottom panel) emitted in the decay of  $^{111}\text{In}$ . O, proton-induced reactions;  $\Delta$ ,  $^4\text{He}$  reactions.

present interest, includes a small contribution from a precompound process at backward angles. This contribution must be subtracted from the  $(p, p')$  cross section before the data can be analyzed in the manner described below. The magnitude of the precompound cross section is conveniently determined by means of a constant-temperature analysis of the data. The procedure is described in detail elsewhere<sup>4</sup> and, as shown in Table I, amounts to  $\sim 10\%$  of the  $(p, p')$  cross section.

In order to extract the isospin mixing fraction from the data the experimental cross sections, corrected for precompound emission in the case of the  $(p, p')$  reaction, are first recast in the form  $R_{\text{exp}} = \sigma(p, p')\sigma(\alpha, \alpha')/\sigma(p, \alpha)\sigma(\alpha, p)$ . In the absence of isospin conservation this quantity would be unity provided that the angular momentum distributions in the two entrance channels are the same. This condition is merely a restatement of the Bohr independence hypothesis. Since this condition is not met it is necessary to apply a correction for angular momentum differences. This may be conveniently done by evaluating a quantity denoted by  $R_{\text{calc}}$ , which is made up of the same combination of cross sections as  $R_{\text{exp}}$  except that these are now calculated by means of the spin-dependent statistical theory. The calculation is performed for the particular distributions of entrance channel spins of interest as obtained from an optical model calculation. The calculation has been described in detail elsewhere.<sup>10</sup> The calculated spectra require input values for the level density parameter,  $\alpha$ , and the pairing energy,  $\delta$ , of the residual nuclei resulting from neutron, proton, or  $\alpha$  emission. These values are based on the compilation of Gilbert and Cameron<sup>16</sup> but were adjusted to give the best overall fit to the  $(p, \alpha)$ ,  $(\alpha, p)$ , and  $(\alpha, \alpha')$  spectra. One additional free parameter in the calculation is the nuclear moment of inertia, which enters into the calcula-

TABLE I. Experimental cross sections and derived quantities for the  $^{111}\text{In}$  compound nucleus.

Reaction	c.m. energy interval (MeV)	Cross section (mb)
$^{107}\text{Ag}(\alpha, p)$	3.0–11.0	$30.3 \pm 4.0$
$^{107}\text{Ag}(\alpha, \alpha')$	8.0–15.5	$7.3 \pm 1.1$
$^{110}\text{Cd}(p, \alpha)$	8.0–15.5	$5.6 \pm 0.5$
$^{110}\text{Cd}(p, p')$	3.0–11.0	$74.0 \pm 7.0$ $68.4 \pm 7.0^a$

$$R_{\text{exp}} = 2.93 \pm 0.57, \quad R_{\text{calc}} = 1.72 \pm 0.09$$

$$G = 1.70 \pm 0.34, \quad G_{\text{max}} = 3.43$$

<sup>a</sup> Compound nuclear cross section.

tion of the level densities. The detailed effect of  $\mathcal{J}$  on the calculated spectra has been described elsewhere.<sup>5</sup> While in previous comparisons for compound nuclei in the  $A \sim 50-70$  mass region<sup>4-7</sup> a value of  $\mathcal{J} = \mathcal{J}_{\text{rigid}}$  was found to give the best overall agreement, it was necessary in the present case to reduce  $\mathcal{J}$  to  $0.25 \mathcal{J}_{\text{rigid}}$  in order to obtain the indicated agreement. The effect of this reduction in  $\mathcal{J}$  on the calculated spectra is to increase the magnitude of the  $(\alpha, \alpha')$  cross section by about a factor of 2 while leaving all the other cross sections virtually unchanged. This effect can be ascribed to the fact that a reduction in  $\mathcal{J}$  leads to a lower density of high-spin states in the residual nucleus. These states are more heavily populated in  $\alpha$ -induced reactions because of the higher angular momentum of the compound nucleus formed in this manner. A reduction in the density of these states favors the emission of particles that are most effective in removing angular momentum from the compound nucleus, i.e.,  $\alpha$  particles. It is unclear at present why the  $^{107}\text{Ag}(\alpha, \alpha')$  reaction requires a reduced value of  $\mathcal{J}$  while similar reactions in the  $A = 50-70$  mass region do not. Fur-

ther work is needed to determine whether this is an isolated case or whether it is indicative of a more general trend.

The experimental and calculated differential cross sections are compared in Fig. 3. The insert to the figure lists the adopted values of  $a$  and  $\delta$ . It is seen that the calculation adequately matches the peak energy and cross section of the above three reactions. The overall shapes of the curves are less adequately reproduced, particularly in the case of the  $(\alpha, p)$  reaction, where the calculated curve is substantially narrower irrespective of the choice of parameters. It may also be noted that the calculated  $(p, p')$  cross section is substantially smaller than the experimental one. This is, of course, a reflection of the enhancement in the measured  $(p, p')$  cross section due to isospin conservation.

The values of  $R_{\text{exp}}$  and  $R_{\text{calc}}$  are listed in Table I. The uncertainty in  $R_{\text{exp}}$  is based on the random errors in the cross sections while that in  $R_{\text{calc}}$  is a measure of the effect of reasonable variations in the various parameters in the calculation. The ratio of  $R_{\text{exp}}$  to  $R_{\text{calc}}$  is designated  $G$  and is also

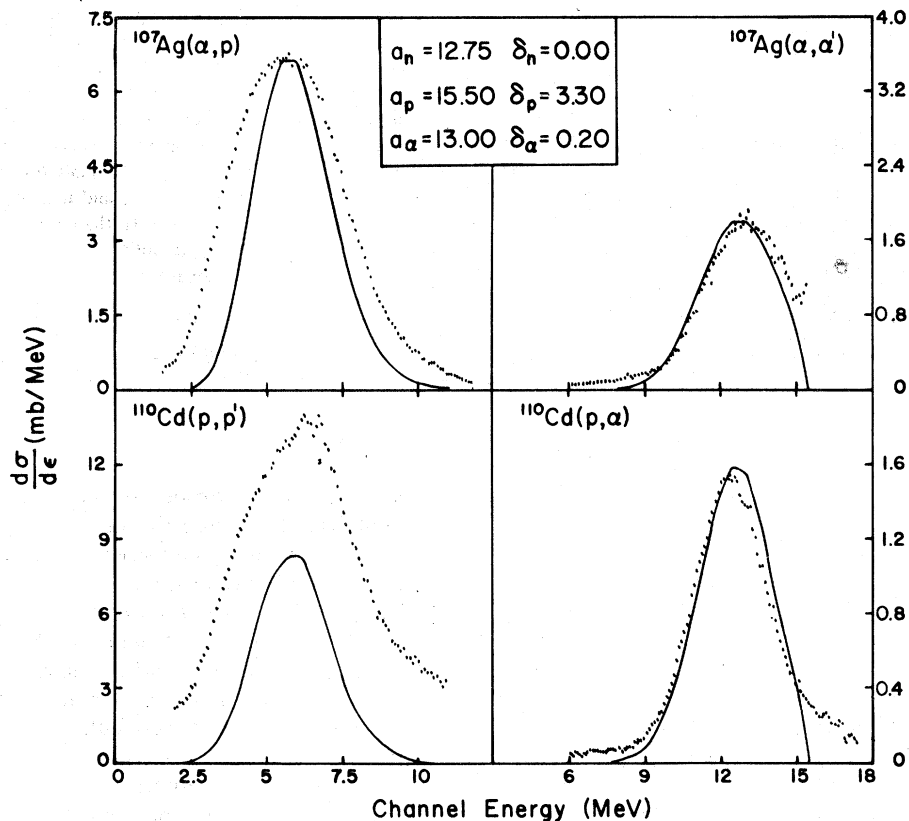


FIG. 3. Comparison of experimental (points) and calculated (curves) energy spectra of protons and  $\alpha$  particles emitted in the decay of  $^{111}\text{In}$ . The calculated spectra are based on the listed  $a$  and  $\delta$  values. The calculation does not include isospin conservation.

listed in Table I. The limiting values of  $G$  are unity, which is obtained if there is complete mixing between the  $T_>$  and  $T_<$  states of the compound nucleus prior to decay, and  $G_{\max}$ , which is the value if there is no mixing.  $G_{\max}$  is calculated by means of the spin- and isospin-dependent statistical theory<sup>10</sup> as described in further detail in the next section. The value of  $G_{\max}$  for the case of present interest is given in Table I. It may be noted that  $G$  lies between the limiting values indicating that partial isospin mixing occurs. We defer a calculation of the mixing fraction to a later section and first proceed to a reformulation of isospin mixing theory.

#### IV. DISCUSSION

##### A. Reformulation of isospin mixing

Previous analyses<sup>3-7,9</sup> of isospin mixing have used relations which include only one factor in the first order (linear) term in the mixing fraction ( $\mu$ ) in the equation relating the measured proton and  $\alpha$  cross sections to this parameter. As will be shown in the present derivation, there are two additional contributions of the same order in  $\mu$ .

The physical Hamiltonian  $H$  is divided into an isospin conserving ( $H_0$ ) and an isospin violating ( $H_1$ ) part. Then, let the wave functions  $\psi_i^<$  and  $\psi_k^>$  denote the eigenfunctions of  $H_0$ , such that the  $\psi_i^<$  have isospin equal to that of the ground state ( $T = T_z$ ) and the  $\psi_k^>$  have isospin  $T = T_z + 1$ . These will be states of pure isospin and since they form a complete set, the eigenfunctions of the total Hamiltonian ( $H$ ) may be written

$$\phi_i^< = \alpha_i \psi_i^< + \sum_j^{N^>} \beta_{ij} \psi_j^>, \quad (1)$$

$$\phi_k^> = \gamma_k \psi_k^> + \sum_l^{N^<} \delta_{kl} \psi_l^<. \quad (2)$$

Where, from unitarity,<sup>17</sup>

$$\alpha_i = \left( 1 - \sum_j^{N^>} |\beta_{ij}|^2 \right)^{1/2}, \quad (3)$$

$$\gamma_k = \left( 1 - \sum_l^{N^<} |\delta_{kl}|^2 \right)^{1/2}, \quad (4)$$

and  $N^>$  and  $N^<$  are, respectively, the number of  $T = T_z + 1$  and the number of  $T = T_z$  states in the energy interval of interest. We assume that the nucleus of interest is heavy enough that the density of  $T = T_z$  states is much greater than the density of  $T = T_z + 1$  states and that the energy is high enough that both  $T_z$  and  $T_z + 1$  states are overlapping. In the limit of small mixing, the  $\phi_i^<$  states become the  $\psi_i^<$  states and the  $\phi_k^>$  states be-

come the  $\psi_k^>$  states.

In order to examine the effects of mixing for a large number of levels, we replace  $\beta_{ij}^2$  and  $\delta_{kl}^2$  by their values averaged over  $i$  and  $j$  (or  $k$  and  $l$ ); by unitarity these averages must be equal. Thus, if this average is denoted  $\beta^2$ , Eqs. (3) and (4) become

$$\alpha = (1 - N^> \beta^2)^{1/2}, \quad (5)$$

$$\gamma = (1 - N^< \beta^2)^{1/2}. \quad (6)$$

Since the widths of the states are proportional to the squares of the amplitudes, the widths of the mixed states will be

$$\Gamma_{\phi^<} = (1 - \mu^{\dagger}) \Gamma^< + \mu^{\dagger} \Gamma^>, \quad (7)$$

$$\Gamma_{\phi^>} = (1 - \mu^{\dagger}) \Gamma^> + \mu^{\dagger} \Gamma^<, \quad (8)$$

where  $\mu^{\dagger} = N^> \beta^2$  and  $\mu^{\dagger} = N^< \beta^2$ .

Since  $\mu^{\dagger}$  is constrained to be less than one and the ratio  $N^</N^>$  is in general 50 or larger for nuclei with mass number greater than 40  $\mu^{\dagger} = \mu^{\dagger} / (N^</N^>)$  will be very small. Thus the  $\phi_i^<$  states will still be predominantly  $T = T_z$  even for large values of  $\mu^{\dagger}$ , while for the values of  $\mu^{\dagger}$  observed in the present experiment the  $\phi_k^>$  states have an almost equal mixture of  $T = T_z$  and  $T = T_z + 1$  components.

From perturbation theory, the damping width of the  $>$  states to the  $<$  states is given by

$$\Gamma^{\dagger} = 2\pi |H|^2 \rho^<(E),$$

where  $|H|$  is the average matrix element connecting the two types of states and  $\rho^<(E)$  is the density of  $<$  states. The fraction of the flux in the  $>$  states which mixes with  $<$  states before decay is then  $\Gamma^{\dagger} / (\Gamma^> + \Gamma^{\dagger})$ ; in terms of the previous expressions involving  $\mu^{\dagger}$  this same fraction can be expressed as  $\mu^{\dagger} \Gamma^< / [(1 - \mu^{\dagger}) \Gamma^> + \mu^{\dagger} \Gamma^<]$ . Equating these two expressions and solving for  $\Gamma^{\dagger}$ , we obtain

$$\left( \frac{\mu^{\dagger}}{1 - \mu^{\dagger}} \right) \Gamma^< = \Gamma^{\dagger} = 2\pi |H|^2 \rho^<(E)$$

or

$$H = \left[ \frac{\mu^{\dagger} \Gamma^<}{(1 - \mu^{\dagger}) 2\pi \rho^<(E)} \right]^{1/2}. \quad (9)$$

Experimentally, the effects of isospin mixing are observed through measurements of the proton and  $\alpha$  branching ratios from compound nuclei formed by proton and  $\alpha$  bombardments. As indicated in the last section these are expressed in terms of parameter  $G$ , which is given by

$$G = 1 + \sigma^{\gamma}(p, p') / \sigma^<(p, p'). \quad (10)$$

In the limit of no isospin mixing the maximum value of  $G$ , denoted by  $G_{\max}$ , is obtained and in this case

$$\frac{\sigma^>(p, p')}{\sigma^<(p, p')} = \frac{T_p^> \Gamma_p^> / \Gamma^>}{T_p^< \Gamma_p^< / \Gamma^<} = \frac{1}{2T} \frac{1}{\Gamma_p^< / \Gamma^<}. \quad (11)$$

Here  $\sigma^>(p, p')$  and  $\sigma^<(p, p')$  denote the cross sections for  $(p, p')$  compound nuclear reactions proceeding through analog ( $T_p^>$ ) and nonanalog ( $T_p^<$ ) intermediate states, respectively.  $T_p^>$  and  $T_p^<$  are the corresponding proton transmission coefficients in the two isospin channels,  $\Gamma_p^>$  ( $\Gamma_p^<$ ) and  $\Gamma^>$  ( $\Gamma^<$ ) are the proton decay width and total decay width, respectively, for analog (nonanalog) states, and  $T$  is the isospin of the proton reaction target. To obtain the last expression in Eq. (11) it has been assumed that  $T_p = (1/2T)T_p^<$  and that  $\Gamma^> \cong \Gamma_p^>$ .

In the present derivation the detailed angular momentum dependence of  $G$  is suppressed and an average value is used. A more exact analysis would allow for the possibility that isospin mixing might be a function of the angular momentum of the compound nuclear state. This derivation could be easily generalized to such a situation by replacing all widths for  $>$  and  $<$  states by the corresponding values for a specific  $J$  and then evaluating  $\mu$  for that  $J$ . A comparison of proton and  $\alpha$ -induced cross sections, however, does not allow the determination of more than one mixing parameter, so the possible angular momentum dependence of

$\mu$  has been ignored.

To obtain  $T_p^>$  and  $T_p^<$  in the case where mixing is allowed, the widths  $\Gamma_{\phi^>}$  and  $\Gamma_{\phi^<}$  are expanded using Eqs. (7) and (8) (where the transmission coefficient after mixing is denoted  $\tau_p$ )

$$\begin{aligned} \tau_p^< &= \frac{2\pi\Gamma_{\phi^<}}{D^<} = \frac{2\pi}{D^<} [\mu^\dagger\Gamma_p^> + (1-\mu^\dagger)\Gamma_p^<] \\ &= 2\pi \left[ \mu^\dagger \frac{\Gamma_p^> D^>}{D^> D^<} + (1-\mu^\dagger) \frac{\Gamma_p^<}{D^<} \right] \\ &= \mu^\dagger \frac{D^>}{D^<} T_p^> + (1-\mu^\dagger) T_p^<. \end{aligned}$$

$D^>$  and  $D^<$  are the average level spacings of analog and nonanalog states, respectively.

But as shown above,  $\mu^\dagger = \mu^\dagger / (N^< / N^>) = \mu^\dagger (D^< / D^>)$ , so

$$\tau_p^< = \mu^\dagger T_p^> + (1-\mu^\dagger) T_p^<$$

and, by symmetry,

$$\tau_p^> = \mu^\dagger T_p^< + (1-\mu^\dagger) T_p^>.$$

If  $D^</D^>$  is denoted  $R_0$ , then these are

$$\tau_p^< = \mu^\dagger T_p^> + (1-R_0\mu^\dagger) T_p^< \quad (12)$$

$$\tau_p^> = \mu^\dagger R_0 T_p^< + (1-\mu^\dagger) T_p^>. \quad (13)$$

Thus,

$$\begin{aligned} \frac{\sigma^>(p, p')}{\sigma^<(p, p')} &= \frac{\mu^\dagger T_p^> + (1-R_0\mu^\dagger) T_p^<}{R_0\mu^\dagger T_p^< + (1-\mu^\dagger) T_p^>} \left( \frac{1}{2T} \right) \frac{[\Gamma_p^>(1-\mu^\dagger) + \Gamma_p^<\mu^\dagger] / [\Gamma^>(1-\mu^\dagger) + \Gamma^<\mu^\dagger]}{[\Gamma_p^<(1-R_0\mu^\dagger) + \Gamma_p^>R_0\mu^\dagger] / [\Gamma^<(1-R_0\mu^\dagger) + \Gamma^>R_0\mu^\dagger]} \\ &= \frac{1}{2T} \frac{1-\mu^\dagger(1-R_0)2T}{1-\mu^\dagger(R_0-1/2T)} \frac{(1-\mu^\dagger) + (\Gamma_p^</\Gamma_p^>)\mu^\dagger}{(1-\mu^\dagger) + (\Gamma^</\Gamma^>)\mu^\dagger} \frac{(1-R_0\mu^\dagger) + (\Gamma^>/\Gamma^<)R_0\mu^\dagger}{(1-R_0\mu^\dagger)(\Gamma_p^</\Gamma^<) + (\Gamma^>/\Gamma^<)R_0\mu^\dagger}, \quad (14) \end{aligned}$$

where  $T_p^>$  has been set equal to  $(1/2T)T_p^<$ . Each factor in Eq. (14) is expanded as a power series in  $\mu^\dagger$  (denoted as  $\mu$  from this point), which gives

$$\begin{aligned} \frac{1}{2T} \frac{1-\mu(1-R_0)2T}{1-\mu(R_0-1/2T)} \\ = \frac{1}{2T} (1_1 A_1 \mu + A_2 \mu^2 + A_3 \mu^3 + \dots), \quad (15) \end{aligned}$$

where

$$A_n = (2T+1)(R_0-1/2T)^n,$$

$$\frac{(1-\mu) + (\Gamma_p^</\Gamma_p^>)\mu}{(1-\mu) + (\Gamma^</\Gamma^>)\mu} = 1 + B_1 \mu + B_2 \mu^2 + B_3 \mu^3 + \dots, \quad (16)$$

where

$$B_n = \left( \frac{1}{R_1} - \frac{\Gamma^<}{R_1 \Gamma_p^<} \right) \left( 1 - \frac{\Gamma^<}{R_1 \Gamma_p^<} \right)^{n-1}$$

and

$$R_1 = \frac{\Gamma_p^>}{\Gamma_p^<} = \frac{1}{2T} \frac{D^>}{D^<},$$

$$\frac{(1-R_0\mu) + (\Gamma^>/\Gamma^<)R_0\mu}{(1-R_0\mu)(\Gamma_p^</\Gamma^<) + (\Gamma^>/\Gamma^<)R_0\mu}$$

$$= \frac{\Gamma^<}{\Gamma_p^<} [1 + C_1 \mu + C_2 \mu^2 + C_3 \mu^3 + \dots], \quad (17)$$

where

$$C_n = R_1 \left( \frac{\Gamma_p^<}{\Gamma^<} - 1 \right) (1-R_1)^{n-1} R_0^n.$$

Thus, combining terms we obtain

$$\begin{aligned} G &= 1 + \frac{\sigma^>(p, p')}{\sigma^<(p, p')} \\ &= 1 + \frac{1}{2T} \frac{\Gamma^<}{\Gamma_p^<} [1 + (A_1 + B_1 + C_1)\mu + \dots]. \quad (18) \end{aligned}$$

In the limit of no mixing,  $\mu = 0$  and the result of Eq. (11) is recovered. Equation (18) relates the experimentally determined value of  $G$  to  $\mu$  and to various constants which are all functions of  $D^>/D^<$ ,  $\Gamma_p^</\Gamma^<$ , and  $T$ . Since these quantities are all calculable it is possible to obtain  $\mu$ . This parameter in turn can be used in Eq. (9) to calculate the isospin mixing matrix element (designated hereafter  $|H_c|$  to conform to previous usage). Equation (18) differs from previous expressions<sup>3-7,9</sup> used to obtain  $\mu$  from  $G$  in that now the  $B_1$  and  $C_1$  terms are included in the coefficient of  $\mu$ . Although Eq. (18) includes higher order terms in  $\mu$ , only the linear term was used in obtaining the values listed in Table II because of the use of first order perturbation theory in deriving  $H_c$  from  $\mu$ .

#### B. Analysis of isospin mixing data

The above formulation may be applied to the previously published data<sup>4-7</sup> as well as to the present results for <sup>111</sup>In in order to obtain the values of  $\mu$  and  $|H_c|$ . The pertinent experimental and calculated quantities are summarized in Table II. The values of  $G_{\max}$  were calculated by means of Eqs. (10) and (11) while those of  $\Gamma_p^</\Gamma^<$  were obtained from a spin-dependent statistical model calculation. As reported in previous publications<sup>4-7</sup> the various parameters in the calculation were adjusted to yield the best overall agreement with the experimental spectra. The level densities of the  $T_<$  and  $T_>$  states of the compound nucleus were evaluated by means of an expression based on the Fermi-gas model<sup>18</sup> at the appropriate

effective excitation  $U_{\text{eff}}$  and for the most probable spin of the compound nucleus  $J_{\text{mp}}$ . The value of  $U_{\text{eff}}$  for the  $T_<$  states is simply  $U_{\text{CN}} - \delta$ , where  $\delta$  is the pairing energy of the compound nucleus while for the  $T_>$  states  $U_{\text{eff}} = U_{\text{CN}} - \Delta - \delta$ , where  $\Delta$  is the energy of the analog state. The experimental spectra are not sensitive to  $a$  or  $\delta$  of the compound nucleus and we have used the values compiled by Gilbert and Cameron<sup>16</sup> in the evaluation of  $\rho$ . The parameters used in the evaluation of  $\rho^>$  are those for the analog nucleus.

The tabulated  $\mu$  values were obtained by means of the linear term in Eq. (18). The listed uncertainties are based on those in the experimental values of  $G$ . In addition, any errors in the calculated values of  $D^>/D^<$  ( $= \rho^</\rho^>$ ) and  $\Gamma_p^</\Gamma^<$  lead to additional uncertainties in  $\mu$ . While the absolute values of the level densities must be fairly uncertain the ratio of  $\rho^</\rho^>$  is much less so. We estimate an uncertainty of  $\sim 50\%$  in this ratio on the basis of reasonable variations in the assumed values of  $a$  and  $\delta$ . This translates itself into a  $\sim 10\%$  uncertainty in  $\mu$ . The values of  $\Gamma_p^</\Gamma^<$  are accurate to within  $\sim 10\%$  since the experimental cross sections are in most cases inconsistent with any larger variations in this quantity. A 10% error leads to a  $\sim 15\%$  uncertainty in  $\mu$ .

The values of  $\mu$  range from 0.16 to 0.62 indicating that isospin mixing occurs to a substantial extent. It appears from the results for <sup>64</sup>Zn and <sup>69</sup>Ga that, for a given nuclide,  $\mu$  decreases with increasing energy. Presumably this trend reflects the fact that the lifetime of the compound nucleus decreases with increasing energy so that there is

TABLE II. Parameters derived in isospin mixing analysis.

Compound nucleus	$U_{\text{CN}}$ (MeV)	$G$	$G_{\max}^a$	$\Gamma_p^</\Gamma^<$	$\rho^<(U_{\text{eff}}, J_{\text{mp}})$ (keV <sup>-1</sup> )	$\rho^>(U_{\text{eff}}, J_{\text{mp}})$ (keV <sup>-1</sup> )	$\mu$	$\Gamma^<(J_{\text{mp}})$ (keV)	$ H_c $ (eV)
<sup>49</sup> V	20.5	2.44 ± 0.45	2.98	0.126	2.01 × 10 <sup>2</sup>	2.17	0.16 ± 0.16	10.5	40 ± 28
<sup>52</sup> Cr	24.2	2.10 ± 0.16	3.02	0.0990	2.26 × 10 <sup>2</sup>	8.05	0.16 ± 0.04	48.9	81 ± 14
<sup>55</sup> Mn	21.8	3.59 ± 0.94	5.27	0.0390	1.23 × 10 <sup>3</sup>	3.78	0.22 ± 0.14	9.47	19 ± 9
<sup>56</sup> Fe	23.9	1.46 ± 0.22	1.98	0.204	4.64 × 10 <sup>2</sup>	10.5	0.32 ± 0.17	22.6	60 ± 31
<sup>60</sup> Ni	23.3	1.58 ± 0.25	2.06	0.188	2.57 × 10 <sup>2</sup>	7.45	0.25 ± 0.16	32.1	81 ± 43
<sup>63</sup> Cu	19.9	1.81 ± 0.39	2.76	0.0946	3.19 × 10 <sup>3</sup>	4.29	0.39 ± 0.19	1.48	6.9 ± 3.8
<sup>64</sup> Zn	17.6	1.16 ± 0.10	1.75	0.267	1.06 × 10 <sup>2</sup>	1.11	0.55 ± 0.12	4.29	89 ± 33
	19.0	1.30 ± 0.13	1.83	0.241	2.57 × 10 <sup>2</sup>	3.39	0.43 ± 0.13	9.62	67 ± 25
	20.5	1.40 ± 0.10	1.85	0.235	6.06 × 10 <sup>2</sup>	9.73	0.35 ± 0.10	19.4	52 ± 15
	22.0	1.45 ± 0.13	1.77	0.260	1.39 × 10 <sup>3</sup>	26.4	0.28 ± 0.14	37.0	41 ± 18
	23.5	1.41 ± 0.10	1.79	0.254	3.36 × 10 <sup>3</sup>	71.1	0.31 ± 0.09	57.3	35 ± 10
<sup>66</sup> Zn	22.7	1.55 ± 0.20	3.13	0.0671	8.44 × 10 <sup>3</sup>	14.6	0.52 ± 0.08	11.4	15 ± 4
<sup>69</sup> Ga	17.4	3.25 ± 0.20	5.27	0.0293	2.92 × 10 <sup>3</sup>	0.535	0.37 ± 0.04	0.752	4.9 ± 0.6
	18.4	2.78 ± 0.14	4.68	0.0340	5.70 × 10 <sup>3</sup>	1.45	0.40 ± 0.04	0.966	4.2 ± 0.5
	20.4	2.61 ± 0.31	3.93	0.0426	2.36 × 10 <sup>4</sup>	9.62	0.34 ± 0.09	1.40	2.2 ± 0.6
	22.4	2.39 ± 0.23	3.30	0.0543	8.14 × 10 <sup>4</sup>	51.9	0.30 ± 0.08	1.98	1.3 ± 0.3
<sup>111</sup> In	20.9	1.70 ± 0.34	3.43	0.0295	6.93 × 10 <sup>7</sup>	974	0.62 ± 0.14	0.0429	0.013 ± 0.004

<sup>a</sup>An error was discovered in the previously reported values of  $G_{\max}$ . The only results which are substantially affected are those for <sup>69</sup>Ga.

less time available for mixing at the higher energies. The increasing complexity of the compound nuclear states at the higher energies may also contribute to this effect. The  $\mu$  values obtained from the present formulation are, on the average, some 30% smaller than those obtained in previous analyses of the data<sup>3-7,9</sup> in which a less complete form of Eq. (18) was used.

The values of  $|H_c|$  were obtained from those of  $\mu$  by means of Eq. (9). The level density of the  $T_\zeta$  states was evaluated for the most probable spin of the compound nucleus in the manner outlined above. The widths of the  $T_\zeta$  states were evaluated by means of the spin-dependent statistical theory for  $J=J_{mp}$ .<sup>4-7</sup> The quoted errors are derived from those tabulated for  $\mu$ . The actual uncertainties must be substantially larger because  $|H_c|$  depends on the actual density of the  $T_\zeta$  levels. It is unlikely that the Fermi-gas model representation can yield absolute level densities with any great degree of accuracy even when the parameters (e.g.,  $a$  and  $\delta$ ) are based on fits to experimental data as they are in the compilation by Gilbert and Cameron.<sup>16</sup> We estimate on the basis of realistic uncertainties in the values of these parameters that the  $|H_c|$  suffer from an absolute uncertainty of about a factor of 2. In spite of this uncertainty the results are of considerable interest since experiments of this type are presently the only source of isospin mixing matrix elements at high excitation energies.

The body of data summarized in Table II is sufficiently large to permit an identification of the factors that determine the magnitude of  $|H_c|$ . The most readily apparent trend is that, for a given

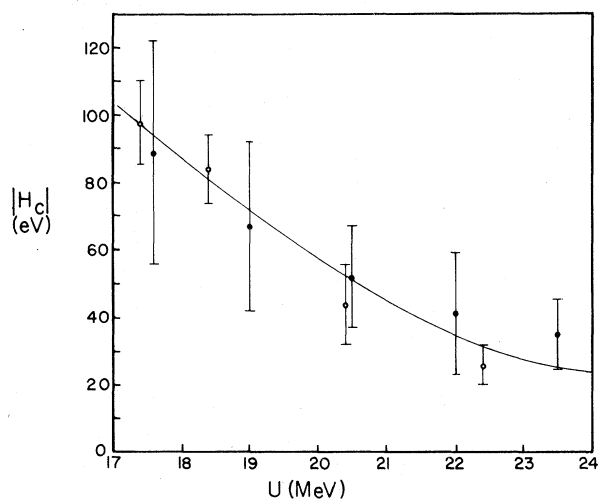


FIG. 4. Energy dependence of  $|H_c|$  for  $^{64}\text{Zn}$  (closed points) and  $^{69}\text{Ga}$  (open points). The  $^{69}\text{Ga}$  values have been increased by a factor of 20.

nucleus,  $|H_c|$  decreases with increasing energy. The results for  $^{64}\text{Zn}$  and  $^{69}\text{Ga}$  are shown in Fig. 4 and it is clear that the matrix elements of both nuclides vary in essentially the same way. The rather strong inverse dependence observed at the lowest energies is consistent with results obtained at energies below 5 MeV. Bloom<sup>19</sup> has tabulated  $|H_c|$  values derived from  $\beta$  decay studies. The results fluctuate widely from one nucleus to another but lie mostly in the 1-40 keV range. The present values extrapolate into the keV range at low energies and so tie in rather well with the  $\beta$  decay data.

It has been previously noticed<sup>9</sup> that the isospin mixing matrix element appears to depend on the value of  $\Gamma_p^</math>/ $\Gamma^<$  and perhaps also on mass number. In order to unravel these effects the  $|H_c|$  were first corrected to a common excitation energy (22 MeV) by means of the curve in Fig. 4. The dependence of  $|H_c|$  on  $\Gamma_p^</math>/ $\Gamma^<$  for those nuclides lying in rather narrow mass intervals (49-60 and 63-69) is shown in Fig. 5. The trends are shown by the straight lines which represent least-squares fits to the data. An additional constraint imposed on these lines is that  $|H_c| \geq 0$ . Although the data exhibit considerable scatter there appears to be a definite correlation between  $|H_c|$  and the proton branching ratio. This behavior presumably reflects the fact that only the proton channel is coupled to both the  $T_\zeta$  and  $T_\zeta$  isospin values. If mixing is caused by the Coulomb inter-$$

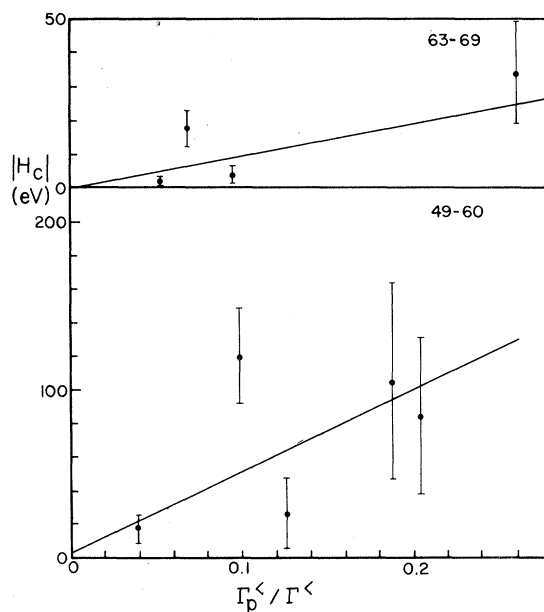


FIG. 5. Dependence of  $|H_c|$  on the proton branching ratio of the  $T_\zeta$  states ( $\Gamma_p^</math>/ $\Gamma^<$ ) for nuclei in the indicated mass intervals. The straight lines represent least-square fits.  $|H_c|$  has been evaluated at 22 MeV.$



action it should be largest in the region where the nuclear force is small and the Coulomb force is large, i.e., in the diffuse nuclear surface. The observed trend suggests that the amount of proton wave function in this region of the nucleus is correlated with the proton decay width. This interpretation is consistent with the analysis by Robson<sup>20</sup> in which isospin mixing is shown to occur in the "external" region.

Having established the dependence of  $|H_c|$  on energy and  $\Gamma_p^</math>/ $\Gamma^<$  we now turn to the mass dependence. Our new result for <sup>111</sup>In provides the evidence. The  $|H_c|$  values in each of the above two mass intervals were evaluated at  $\Gamma_p^</math>/ $\Gamma^<$  = 0.0295, the value appropriate to the <sup>111</sup>In compound nucleus, and the results are shown in Fig. 6. On the basis of the limited available data it appears that  $|H_c|$  decreases rather sharply with increasing  $A$ . This trend appears to be consistent with the occurrence of mixing in the "external" region since the fraction of nucleons at the surface decreases with increasing  $A$ . The observed effect does appear to be larger than expected on this basis but the data are sparse and uncertain. If further measurements bear out such a strong trend it will be necessary to invoke other factors. One possibility is that the complexity of the compound nuclear states increases with  $A$  leading to a similar effect as an increase in energy.$$

It is interesting to note that the mass dependence at 22 MeV differs from that obtained from beta decay measurements.<sup>19</sup> The latter yield Coulomb matrix elements that fluctuate widely from one nucleus to another and display no apparent systematic mass dependence. In that case, however, mixing occurs between discrete  $T_>$  and  $T_<$  levels whose overlap is sensitive to the particular configurations involved.

## V. CONCLUSIONS

We have measured the extent of isospin mixing in <sup>111</sup>In at 20.9 MeV and determined the values of

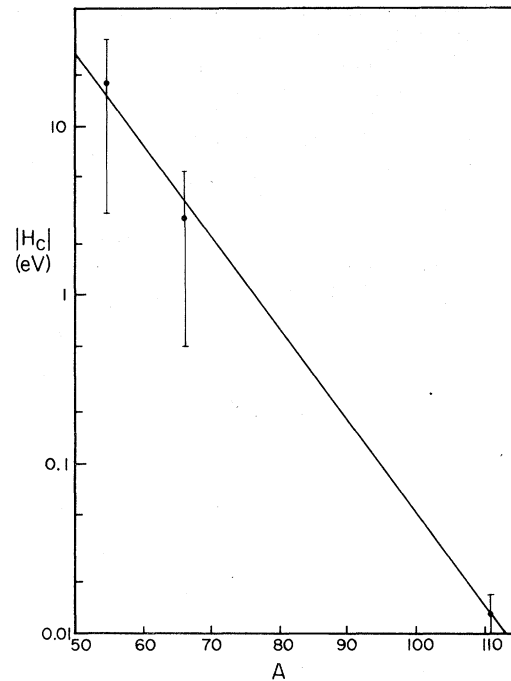


FIG. 6. Dependence of  $|H_c|$  on  $A$ .  $|H_c|$  has been evaluated at 22 MeV and for  $\Gamma_p^</math>/ $\Gamma^<$  = 0.0295.$

the mixing fraction  $\mu$  and the isospin mixing matrix element  $|H_c|$ . Their respective values are  $0.62 \pm 0.14$  and  $0.013 \pm 0.004$  eV. The theory of isospin mixing has been reformulated to include additional terms in the relation between  $\mu$  and the measured cross sections. The previous data available in the  $A \sim 50-70$  mass region were reanalyzed with the new formalism in order to obtain the values of  $|H_c|$ . It is found that  $|H_c|$  increases with the proton emission branching ratio of  $T_<$  states and varies inversely with excitation energy and mass number.

We would like to thank Dr. J. C. Pacer and Dr. J. R. Wiley for their assistance throughout the tandem runs.

\*Work supported by the U. S. Energy Research and Development Administration.

<sup>1</sup>M. J. Fluss, J. M. Miller, J. M. D'Auria, N. Dudev, B. M. Foreman, L. Kowalski, and R. C. Reedy, Phys. Rev. **187**, 1449 (1969).

<sup>2</sup>S. M. Grimes, J. D. Anderson, A. K. Kerman, and C. Wong, Phys. Rev. C **5**, 85 (1972).

<sup>3</sup>L. C. Vaz, C. C. Lu, and J. R. Huizenga, Phys. Rev. C **5**, 463 (1972).

<sup>4</sup>J. Wiley, J. C. Pacer, C. R. Lux, and N. T. Porile, Nucl. Phys. **A212**, 1 (1973).

<sup>5</sup>N. T. Porile, J. C. Pacer, J. Wiley, and C. R. Lux,

Phys. Rev. C **9**, 2171 (1974).

<sup>6</sup>N. T. Porile, C. R. Lux, J. C. Pacer, and J. Wiley, Nucl. Phys. **A240**, 77 (1975).

<sup>7</sup>C. R. Lux and N. T. Porile, Nucl. Phys. **A248**, 441 (1975).

<sup>8</sup>S. M. Grimes, Phys. Rev. C **11**, 253 (1975).

<sup>9</sup>N. T. Porile and S. M. Grimes, Phys. Rev. C **11**, 1567 (1975).

<sup>10</sup>A. J. Kennedy, J. C. Pacer, A. Sprinzak, J. Wiley, and N. T. Porile, Phys. Rev. C **5**, 500 (1972).

<sup>11</sup>A. Sprinzak, A. J. Kennedy, J. C. Pacer, J. Wiley, and N. T. Porile, Nucl. Phys. **A203**, 280 (1973).

<sup>12</sup>F. S. Goulding, D. A. Landis, J. Cerny, and R. M. Pehl, Nucl. Instrum. **31**, 1 (1964).

<sup>13</sup>Obtained from Oak Ridge National Laboratory.

<sup>14</sup>C. F. Williamson, J. P. Boujot, and J. Picard, Saclay, Report No. CEA-R3042, 1966 (unpublished).

<sup>15</sup>A. J. Kennedy, J. Pacer, A. Sprinzak, J. Wiley, and N. T. Porile, Nucl. Instrum. **101**, 471 (1972).

<sup>16</sup>A. Gilbert and A. G. W. Cameron, Can. J. Phys. **43**, 1446 (1965).

<sup>17</sup>Because these states have a decay width, they have complex wave functions whose modulus decreases with time as  $\exp(-\Gamma t/\hbar)$ . The flux which "disappears" from

the excited states is found in the particle-plus-residual nucleus channel, so that unitarity is not violated. It is therefore necessary to normalize the wave function to one at time zero, even though the modulus decreases with time.

<sup>18</sup>C. C. Lu, L. C. Vaz, and J. R. Huizenga, Nucl. Phys. **A190**, 229 (1972).

<sup>19</sup>S. D. Bloom, in *Isobaric Spin in Nuclear Physics*, edited by J. D. Fox and D. Robson (Academic, New York, 1966), p. 123.

<sup>20</sup>D. Robson, Phys. Rev. **137**, B 535 (1965).